Ecosystems (2006) 9: 673–688
DOI: 10.1007/s10021-006-0029-x

ECOSYSTEMS

Carbon Dioxide Dynamics and Controls in a Deep-water Wetland on the Qinghai-Tibetan Plateau

Mitsuru Hirota,[1]* Yanhong Tang,[1] Qiwu Hu,[2] Shigeki Hirata,[3] Tomomichi Kato,[4] Wenhong Mo,[5] Guangmin Cao,[2] and Shigeru Mariko[5]

[1]*National Institute for Environmental Studies, Onogawa 16-2, Tsukuba, Ibaraki 305-8506, Japan;* [2]*Northwest Plateau Institute of Biology, Chinese Academy of Science, Xining, 810001, People's Republic of China;* [3]*Graduate School of Life and Environmental Sciences, University of Tsukuba, Tsukuba, Ibaraki 305-8572, Japan;* [4]*Frontier Research Center for Global Change, 3173-25 Showa-machi, Kanazawa-ku, Yokohama City, Kanagawa 236-0001, Japan;* [5]*Institute of Biological Sciences, University of Tsukuba, Tsukuba, Ibaraki 305-8572, Japan*

Abstract

To initially characterize the dynamics and environmental controls of CO_2, ecosystem CO_2 fluxes were measured for different vegetation zones in a deep-water wetland on the Qinghai-Tibetan Plateau during the growing season of 2002. Four zones of vegetation along a gradient from shallow to deep water were dominated, respectively by the emergent species *Carex allivescens* V. Krez., *Scirpus distigmaticus* L., *Hippuris vulgaris* L., and the submerged species *Potamogeton pectinatus* L. Gross primary production (GPP), ecosystem respiration (Re), and net ecosystem production (NEP) were markedly different among the vegetation zones, with lower Re and GPP in deeper water. NEP was highest in the *Scirpus*-dominated zone with moderate water depth, but lowest in the *Potamogeton*-zone that occupied approximately 75% of the total wetland area. Diurnal variation in CO_2 flux was highly correlated with variation in light intensity and soil temperature. The relationship between CO_2 flux and these environmental variables varied among the vegetation zones. Seasonal CO_2 fluxes, including GPP, Re, and NEP, were strongly correlated with aboveground biomass, which was in turn determined by water depth. In the early growing season, temperature sensitivity (Q_{10}) for Re varied from 6.0 to 8.9 depending on vegetation zone. Q_{10} decreased in the late growing season. Estimated NEP for the whole deep-water wetland over the growing season was 24 g C m^{-2}. Our results suggest that water depth is the major environmental control of seasonal variation in CO_2 flux, whereas photosynthetic photon flux density (PPFD) controls diurnal dynamics.

Key words: alpine ecosystem; aquatic plants; NEP; water depth; wetland; zonal vegetation.

Introduction

High-latitude wetlands in the northern hemisphere are thought to play a key role in controlling the global carbon cycle for two main reasons. First, high-latitude wetlands cover a vast area, approximately 192–500 $\times$ 10^6 ha, and contain a large amount of organic carbon, ranging from 200–455 $\times$ 10^{15} g, that accounts for approximately one-third of the global soil carbon (Gorham 1991; Turunen and others 2002). The high soil carbon storage in high-latitude wetlands is probably caused by relatively moderate decomposition rates under cool and waterlogged anaerobic conditions compared to rates of primary productivity (Trumbore and others 1999). Second, carbon dynamics in high-latitude

Received 10 March 2005; accepted 14 September 2005; published online 1 June 2006.
*Corresponding author; e-mail: hirota.mitsuru@nies.go.jp; deepblue2jp@yahoo.co.jp

wetland ecosystems are thought to respond dramatically to climate changes, such as the temperature and precipitation changes that are predicted to occur under global warming conditions (Oechel and others 1993; IPCC 2001). These wetland ecosystems, which have been a major sink for atmospheric carbon since the last deglaciation, may therefore greatly alter levels of atmospheric carbon in the future because of modified productivity and decomposition rates.

A recent General Circulation Model (GCM) has suggested significant polar amplification of 2–6°C in the circum-arctic region by global warming over the next 100 years (IPCC 2001). This could potentially cause large-scale changes in the carbon dynamics of high-latitude wetland ecosystems and consequently affect the global carbon cycle. Carbon dynamics in high-altitude wetlands will also be sensitive to climate variation for similar reasons. However, our understanding of carbon dynamics in high-altitude wetlands is very limited (Wickland and others 2001). We therefore chose to investigate wetlands in one of the largest and highest alpine ecosystems in the world, the Qinghai-Tibetan Plateau.

The Qinghai-Tibetan Plateau (av. 4000 m a.s.l.) is the largest geographical unit on the Eurasian continent, containing many lakes and wetlands of considerable size (ca. 5 ha; Zhao 1999). The organic content of the alpine wetland soil is the highest of all the plateau ecosystems in the world (Wang and others 2002). The climate of this region is characterized by long, cold winters and short, cool summers with abundant light and relatively high precipitation. The abundant light and relatively humid climate during the growing season could lead to high productivity and an increase in organic carbon in the soil. On the other hand, the carbon decomposition rate may also be high because of the rich organic carbon load in the soil. It is thus necessary to elucidate growing season CO_2 fluxes to understand the carbon dynamics of alpine wetlands.

Large spatial variability in carbon dynamics has been observed in northern wetlands (Alm and others 1997; Bubier and others 1999; Joiner and others 1999; Christensen and others 2000). This spatial variability could be crucial to our understanding of the carbon budget and its underlying mechanisms (Waddington and Roulet 1996; Heikkinen and others 2004). Geographical and climatic factors will cause large-scale variation in carbon dynamics, while environmental heterogeneity at local or microsite scales will cause considerable local-scale variation in the carbon cycle (Alm and others 1997; Bubier and others 1998, 2003; Waddington and Roulet 2000). Most wetlands surrounding lakes and rivers are characterized by an environmental gradient caused by water availability and soil environment. Along this environmental gradient from the water body to the upland, a transition in the vegetation is usually observed (Mitsch and Gosselink 2000). We expected that differences in the wetland environment and vegetation along a water-depth gradient would result in spatial differences in carbon dynamics.

We previously reported that high spatial and temporal variation in growing season CH_4 flux in an alpine wetland on this plateau was controlled by vegetation structure (Hirota and others 2004). Here, we hypothesized that water depth will be the major environmental factor affecting CO_2 flux, that is, gross primary production (GPP), ecosystem respiration (Re), and net ecosystem production (NEP), in different vegetation zones. Our major aims were to clarify the dynamics of the CO_2 fluxes for different vegetation zones in a typical deep-water wetland on the Qinghai-Tibetan plateau; and to address how environmental and vegetation variables control CO_2 fluxes.

Methods

Site Description

The study site was located in the Luanhaizi wetland (latitude 35°55.5′N, longitude 101°20.7′E, 3,250 m a.s.l., ca 20 ha) on the Qinghai-Tibetan Plateau (Figure 1). The climate is characterized by low temperatures and limited precipitation. The annual average temperature and precipitation for 1981–2000 were: −1.7°C (ranging from −15°C in January to 10°C in July) and 561 mm.

In 2002, the site was flooded at an average water depth of 25 cm over the main growing season from July to September. The water was classified as oligosaline (conductance = 0.7–5.2 mS cm^{-1}; Cowardin and others 1979) and alkaline (pH = 8.5–10.1). The wetland is considered mesotrophic, with total dissolved inorganic nitrogen content in water of 0.1–0.3 mg L^{-1} (Vollenweider 1968).

In the wetland, three emergent plant zones were dominated by *Carex allivescens* V. Krez. (*ZCar*), *Scirpus distigmaticus* L. (*ZSci*), or *Hippuris vulgaris* L. (*ZHip*), and one submerged plant zone was dominated by *Potamogeton pectinatus* L. (*ZPot*) along a gentle gradient from shallow to deep water. *ZCar* comprised 3.4% of the study area, *ZSci* 20.5%, *ZHip* 2.6%, and *ZPot* 73.5% (M. Hirota and others, unpublished data). Detailed information is given in Table 1.

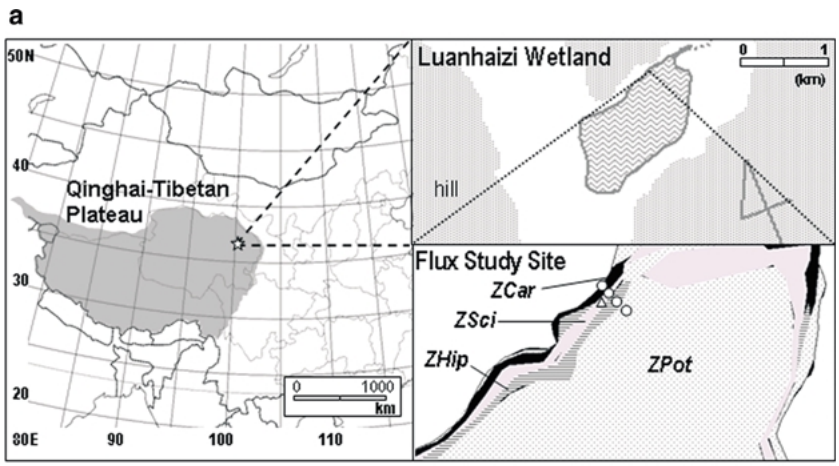

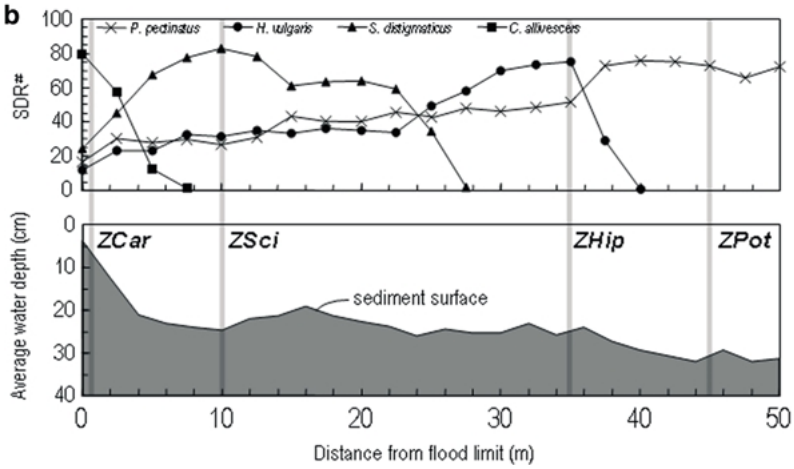

Figure 1. **a** Location of the Luanhaizi wetland. The *cross* represents the meteorological tower; *open circles* indicate the locations of flux measurements; the dashed line indicates a stream. **b** Vegetation distribution of dominant aquatic plants by an summed dominance ratio (SDR) index and a schematic cross-section from the flood-line. *Gray lines* indicate the location of flux measurements in each zone. The SDR index was calculated from vegetation relative cover (RC) and relative height above the soil surface (RH) as SDR = (RC + RH)/2.

Environmental Measurements

A meteorological tower equipped with a data logger (Thermic 2300A, Eto Denki Ltd, Tokyo) was placed in the middle of the mosaic area between *ZSci* and *ZHip* at the northwestern edge of the wetland (Figure 1). We monitored temporal changes in air temperature, water temperature at a depth of 10 cm, soil temperature at a depth of 5 cm, and photosynthetic photon flux density (PPFD) above and below the water surface (air temperature, MT-060, Eko Instruments, Tokyo; water and soil temperature, TidbiT TBI32-20+50, StowAway, Bourne, MA; PPFD, ML-020P, Eko Instruments, Tokyo). Meteorological measurements were recorded every 10 min from July to mid-September 2002. Water depth was measured next to the tower every day. Precipitation data were obtained from a station of the Chinese Academy of Sciences.

Vegetation Biomass

We set one chamber in each vegetation zone. In the chamber, we monitored temporal changes in the aboveground biomass of plants. Three of the zones (other than *ZPot*) had mixed vegetation composed of several species (Table 1). Aboveground biomass was expressed as the sum of the biomass of all species in the chamber. The biomass of each species was calculated by multiplying the number of shoots at the time of flux measurement by biomass per shoot. After the final flux measurement, we harvested aboveground tissue of all live plants in the chamber.

CO_2 Flux Measurements

We used two methods to measure flux from early July to mid-September 2002. The static chamber technique (Hirota and others 2004) measures CO_2 and CH_4 flux, and the dynamic chamber technique (Waddington and Roulet 1996) measures CO_2 flux using a portable infrared gas analyzer (LI-800, LiCor Inc., Lincoln, NE, USA). We used the same chamber system for both types of measurements. For more information on the chamber system, see Hirota and others (2004).

Table 1. Species Component with Biomass, Water Depth, and Depth of Organic Layer in the Four Vegetation Zones

Zone	Vegetation	Relative biomass[a] (%)	Total biomass[a] (g DW m^{-2})	Mean water depth[b] (cm)	Depth of organic layer[c] (cm)
ZPot	*Potamogeton pectinatus* L.[d]	100	120	27 (14–38)	7 (3)
	Hippuris vulgarisl L.	0			
	Scirpus distigmaticus L.	0			
	Carex allivescers V. Krez.	0			
ZHip	*Hippuris vulgaris* L.[d]	85	393	24 (13–33)	33 (6)
	Potamogeton pectinatus L.	15			
	Scirpus distigmaticus L.	0			
	Carex aliivescers V. Krez.	0			
ZSci	*Scirpus distigmaticus* L.[d]	80	412	19 (9–25)	66 (12)
	Hippuris vulgaris L.	13			
	Potamogeton pectinatus L.	7			
	Carex allivescers V. Krez.	0			
ZCar	*Carex allivescens* V. Krez[d]	88	384	12 (1–20)	78 (7)
	Hippuris vulgaris L.	5			
	Scirpus distigmaticus L.	4			
	Potamogeton pectinatus L.	3			

[a]*Mean values during the measurement period.*
[b]*Mean and range of water depth, minimum and maximum values, during the measurement period.*
[c]*Mean values, which were estimated by distance from sediment surface to clay layer (n = 3).*
[d]*Dominant species.*

We measured NEP under light conditions, and then measured Re under dark conditions by covering the chamber with aluminum foil. These paired measurements were performed seven times throughout the day. A temporary framework was installed as a foothold to avoid shading and soil disturbance during measurement.

CO_2 flux was measured using the static chamber technique at 13:00, 15:00, 17:00, 19:00, 22:00, 1:00, 4:00, 7:00, 9:00, 11:00, and 13:00 (Beijing standard time) on 4, 5 July, 19, 20 July, 25, 26 July, 12, 13 August, 26, 27 August, and 14, 15 September. Gas samples were withdrawn from the chamber headspace at 1, 3, 6, 9, and 12 min after the system was closed. To avoid the bias of long incubation time, we eliminated from analysis the value for 9 and/or 12 min if the linearity was not good enough. Samples were taken using a needle inserted directly into a 5-ml evacuated vial, and then analyzed using a gas chromatograph (GL 390B, GL Science, Tokyo). Injection, detection of TC, and columivoven temperatures were 120°C, 120°C, and 50°C, respectively; pure helium was used as a carrier gas. Gas samples in the vials were stored for 2 months, and then transported by air to the laboratory in Japan. A control test with gas standards (0 and 466 ppm) stored in the same type of vial showed no significant changes in gas concentrations during storage and transportation. Samples were injected into the gas chromatograph using gas-tight syringes (A-2 Type Gas Syringes, Valco Instruments, Houston, TX, USA). Analytical error on duplicate samples was less than 1.8%. Gas standards (0 and 1999 ppmv) were run after every ten duplicate vials. The gas chromatograph had a detection limit of 0.5 ppm. The rate of CO_2 flux was calculated from the linear regression of change in CO_2 concentration in the chamber over time. Only samples with a regression correlation coefficient greater than $R^2 = 0.85$ were used for further analysis. Data with a regression correlation coefficients $R^2 < 0.85$ were excluded, which consisted of 14.4% of the total samples.

CO_2 flux was measured using the dynamic chamber technique on 2, 3 August, 16, 17 August, 26, 27 August, and 14, 15 September. One measurement cycle of 32 min (8 min per chamber) was repeated every 1 h during the daytime and every 3 h during the nighttime. The measuring system comprised one reference line and four identical sample lines, two IRGAs with absolute modes (Li-800, LiCor Inc., Lincoln, NE, USA) and a data logger (NR-1000 with1010, Keyence, Tokyo). The reference and sample lines were pneumatically independent of each other. In this system, ambient air entered the chambers at a flow rate of 3.0–3.2 L

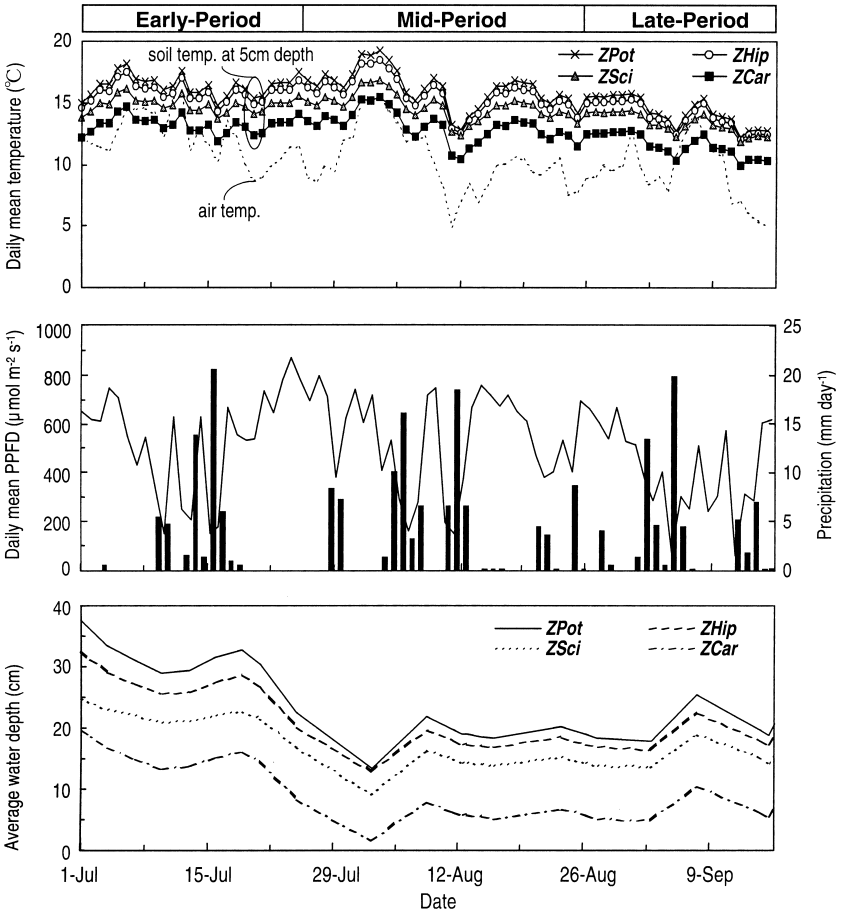

Figure 2. Temporal variation in environmental factors: soil temperature at a depth of 5 cm in each vegetation zone and whole-site daily mean air temperature, photosynthetic photon flux density (PPFD), precipitation, and water depth from 1 July to 15 September 2002.

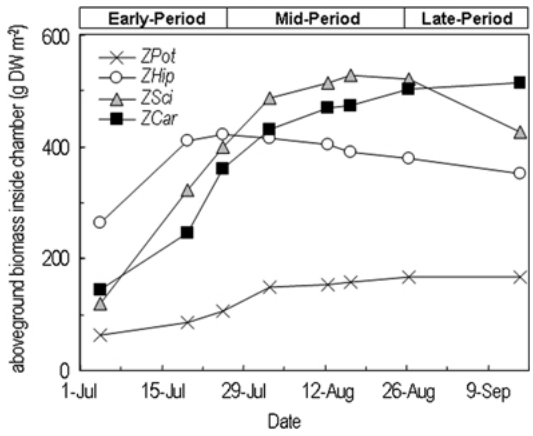

Figure 3. Seasonal variation in aboveground biomass inside chambers for each vegetation zone from 4 July to 15 September 2002.

min^{-1}, CO_2 flux was calculated from the linear change in the differential between the CO_2 concentration of ambient air and of air in the chamber, recorded every 10 s. To examine whether the two methods give consistent results in measuring CO_2 fluxes, we measured the fluxes using the dynamic chamber technique immediately after the sampling by the static technique on 26–28 August, and on 14–15 September. Because the flux data showed no significant differences between the two approaches, we concluded that the observations from the two methods are consistent for the ecosystem.

During the flux measurements, we measured PPFD and air temperature within the chamber, ambient air temperature, water and soil temperatures at a depth of 5 cm, and redox potential (Eh; RM-20P, TOA Electric Co., Tokyo) at soil depths of 5 and 30 cm.

Data Analysis

Hourly measurements of soil temperature in each chamber and incident PPFD at the meteorological tower were used to estimate flux of gross primary production (GPP) and Re from net CO_2 flux (NEP). We adopted the sign convention of ecosystem CO_2 uptake as positive and CO_2 emission via respiration as negative. Firstly, NEP was regressed against

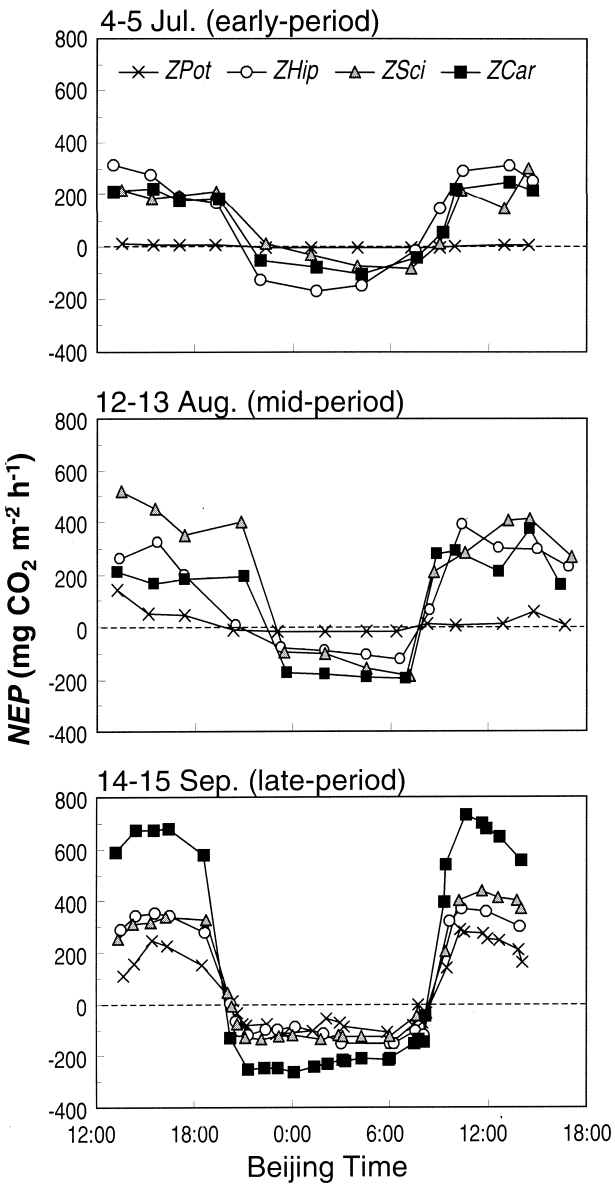

Figure 4. Examples of diurnal variation in net ecosystem production (NEP) for four vegetation zones during different growth periods; 4, 5 July (*top*), 12, 13 August (*center*), and 14, 15 September (*bottom*). Positive and negative values of NEP, respectively represent CO_2 uptake and CO_2 emission.

PPFD using a rectangular hyperbola (Thornley and Johnson 1990) as follows:

$$\mathrm{NEP} = \frac{\alpha \cdot P\mathrm{max} \cdot \mathrm{PPFD}}{\alpha \cdot \mathrm{PPFD} + P\mathrm{max}} + R \qquad (1)$$

where α is the initial slope of the rectangular hyperbola, also called the ''apparent quantum yield'', $Pmax + R$ is the asymptote of NEP, and R is the y-axis intercept, or dark respiration.

Secondly, Re was regressed exponentially against soil temperature at a depth of 5 cm (ST5)

$$\mathrm{Re} = a \times \exp(\mathrm{ST5} \times b) \qquad (2)$$

where a and b are coefficients. The Q_{10} value, which is the change in Re rate over a 10°C change in soil temperature (Raich and Schlesinger 1992) was expressed as follows:

$$Q_{10} = \exp(10 \times b) \qquad (3)$$

Finally, GPP was calculated from Re and NEP as follows:

$$\mathrm{GPP} = \mathrm{NEP} - \mathrm{Re} \qquad (4)$$

To examine environmental controls on seasonally of CO_2 flux, the data were divided into three growth periods (early period: 4–26 July, mid-period: 27 July – 17 August, and late period: 18 August – l5 September). We determined the NEP–PPFD relationship [Eq. (1)] for each measurement day, and the relationship between Re and ST5 [Eq. (2)] for each growth period using KaleidaGraph v3.5 (Synergy Software Inc.). Multiple stepwise regression was used to construct an empirical model of seasonal NEP, Re, and GPP using the measured environmental factors and statistical software (SYSTAT Ver. 10.2). The carbon dynamics of the whole wetland were estimated using data on CO_2 flux and the amount of vegetated area in each zone.

Results

Environmental Variables

Daily mean air and soil temperatures showed a similar seasonal fluctuation (Figure 2). Daily mean soil temperature at a depth of 5 cm varied among the four zones, with *ZPot* > *ZHip* > *ZSci* > *ZCar*. The daily mean air temperature peaked on 15 July, but the daily mean soil temperature in each zone peaked on 2 August. Daily mean PPFD varied from 72 to 885 μmol m^{-2} s^{-1} during the growing season. Rainfall events occurred over the growing season (maximum, 20.6 mm d^{-1}). Water depth decreased gradually, reached the minimum value in each zone on 2 August, and was then restored by rainfall and exhibited only small fluctuations over the rest of the growing season. The water depth was in the order of *ZPot* > *ZHip* > *ZSci* > *ZCar*.

Variation in Plant Biomass

Aboveground biomass increased during the early growing season, but its seasonal variation pat-

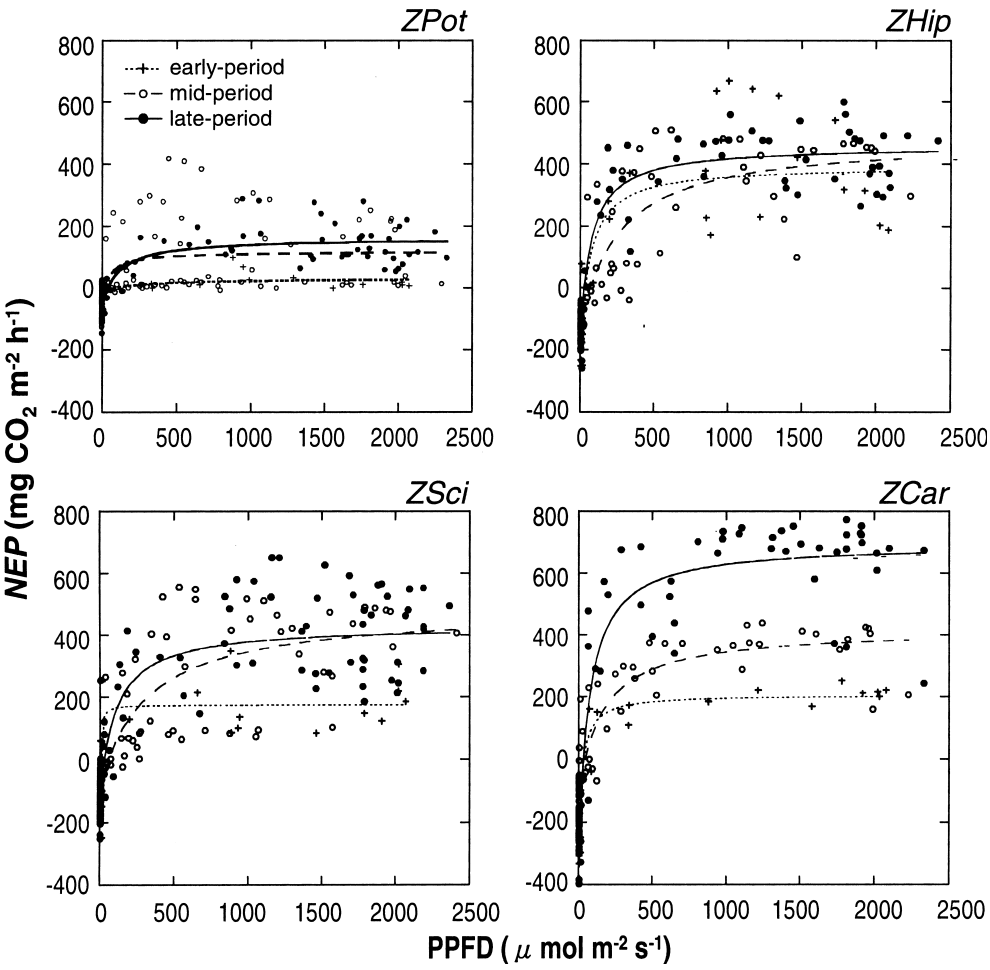

Figure 5. Relationship between PPFD and NEP in four vegetation zones. Positive values indicate net CO_2 uptake. Early period: 4 to 26 July, mid-period: 27 July to 17 August, and late period: 17 August to 15 September. Curves were fitted using the rectangular hyperbola regression from Eq. (1). See Table 2 for a summary of parameter estimates.

terns differed markedly among the vegetation zones (Figure 3). *ZHip* and *ZSci* reached their maximum aboveground biomass in late July and in mid-August, respectively, but *ZPot* and *ZCar* reached their peak biomass in late August and mid-September, respectively. Peak biomass of the submerged plant zone, *ZPot* (173 g DW m^{-2}) was lower than that of the emergent plant zones, *ZHip*, *ZSci*, and *ZCar* (415, 525, and 511 g DW m^{-2}, respectively).

Daily Variation in CO_2 Flux

Net CO_2 flux in the four vegetation zones exhibited similar diurnal patterns but varied in magnitude (Figure 4). All vegetation zones had a positive net CO_2 flux (CO_2 uptake) during the daytime, and CO_2 uptake was highest between 10:00 and 16:00. Negative CO_2 flux (CO_2 emission) occurred between 20:00 and 8:00, with small differences explained by the duration of light availability in the different growth periods. We observed large diurnal variations in net CO_2 flux, but little variation during the night. The range of variation in net CO_2 flux differed markedly among the vegetation zones and increased in the late growth period.

PPFD–saturated NEP (*NEPmax*) throughout the entire period was highest in *ZCar* with 708 mg CO_2 m^{-2} h^{-1}, but smallest in *ZPot*. In *ZPot* and *ZCar*, NEP*max* showed marked seasonal variation and increased from the early period to the late period (Figure 5, Table 2). In the other two vegetation zones, the seasonal pattern of variation in NEP*max* was indistinct or absent (Table 2).

Ecosystem respiration (Re) differed among the vegetation zones and among growth periods (Figure 6). Re was exponentially correlated with soil temperature at a depth of 5 cm (ST5), and soil temperature accounted for approximately 48–88% of variation in Re ($P < 0.05$, Table 3), In *ZPot* and *ZCar*, the Re-temperature correlation differed significantly among the three growth periods (Figure 6, Table 3). Q_{10} was higher in the early period than in the other two periods (Table 3).

Table 2. Nonlinear Net Ecosystem Production-PPFD Rectangular Hyperbola Curve Fit Parameters

Zone	*Pmax* ($mgCO_2\ m^{-2}h^{-1}$)	α gCO_2 ($\mu mol\ photon^{-1}$)	*R* ($mgCO_2\ m^{-2}h^{-1}$)	*n*	r^2
Early period (4 Jul–26 Jul)					
ZPot	40.2	12	−8.99	27	0.68
ZHip	553	658	−160	29	0.86
ZSci	264	1482	−89.7	30	0.76
ZCar	407	1094	−199	28	0.82
Mid-period (2 Aug–17 Aug)					
ZPot	168	299	−50.5	85	0.61
ZHip	596	186	−116	87	0.95
ZSci	562	288	−79.8	88	0.94
ZCar	520	252	−98.1	84	0.94
Late period (26Aug–15 Sep)					
ZPot	215	154	−52.7	104	0.88
ZHip	569	599	−113	99	0.87
ZSci	529	390	−99.5	101	0.90
ZCar	945	967	−243	100	0.88
Entire period (4 Jul–15 Sep)					
ZPot	183	130	−48.6	217	0.44
ZHip	553	282	−123	216	0.87
ZSci	494	425	−85.7	218	0.83
ZCar	708	263	−154	211	0.84

Ranges of R^2 at $P < 0.001$ are applicable for all parameters.

Seasonal Variation in CO_2 Flux

Gross Primary Production (GPP) increased from July to early August and then either decreased or remained high until mid-September, depending on the vegetation zone (Figure 7). Re, however, tended to decrease slightly at the start of the growing season and then stabilized until the end of the growing season. A large decrease in Re occurred on 2–3 August when the water depth and soil temperature reached their lowest and highest levels, respectively, in the growing season (Figures 2 and 7). All NEP values were positive except for that of *ZCar* on 2–3 August.

The daily summed CO_2 flux (GPP, Re, and NEP) was positively correlated to the estimated total aboveground biomass inside the chamber (Figure 8). The daily summed GPP and Re for each zone were respectively negatively and positively correlated with average water depth (Figure 8). The daily summed NEP exhibited no clear relationship with average water depth in each zone. When data from 2–3 August were omitted, stronger relationships between the daily summed CO_2 flux and aboveground biomass or average water depth were detected, especially for the emergent plant zones.

Growing Season CO_2 Flux

To estimate daily GPP and Re, we constructed stepwise-regression models using measured GPP, Re, and the environmental factors PPFD and temperature of air and soil (Table 4). Estimated GPP, Re and NEP were highly correlated to the observed data (Figure 9). GPP and Re in each zone were affected by water depth, but not by PPFD. Daily summed NEP in each zone was calculated from the estimated GPP and Re using Eq. 4. GPP and Re estimated by the regression models coincided well with observed GPP and Re (Figure 9). However, estimated NEP tended to underestimate observed NEP, especially in *Zpot*. The coefficient of determination of the linear regression for NEP was greatest in *ZCar* > *ZSci* > *ZHip* > *ZPot*.

Gross primary production (GPP) and Re decreased as water depth increased with the highest in *ZCar* and the lowest in *ZPot* (Figure 10). During the growing season, the estimated total GPP for the entire wetland was 60.9 g C m^{-2}, and the esti-

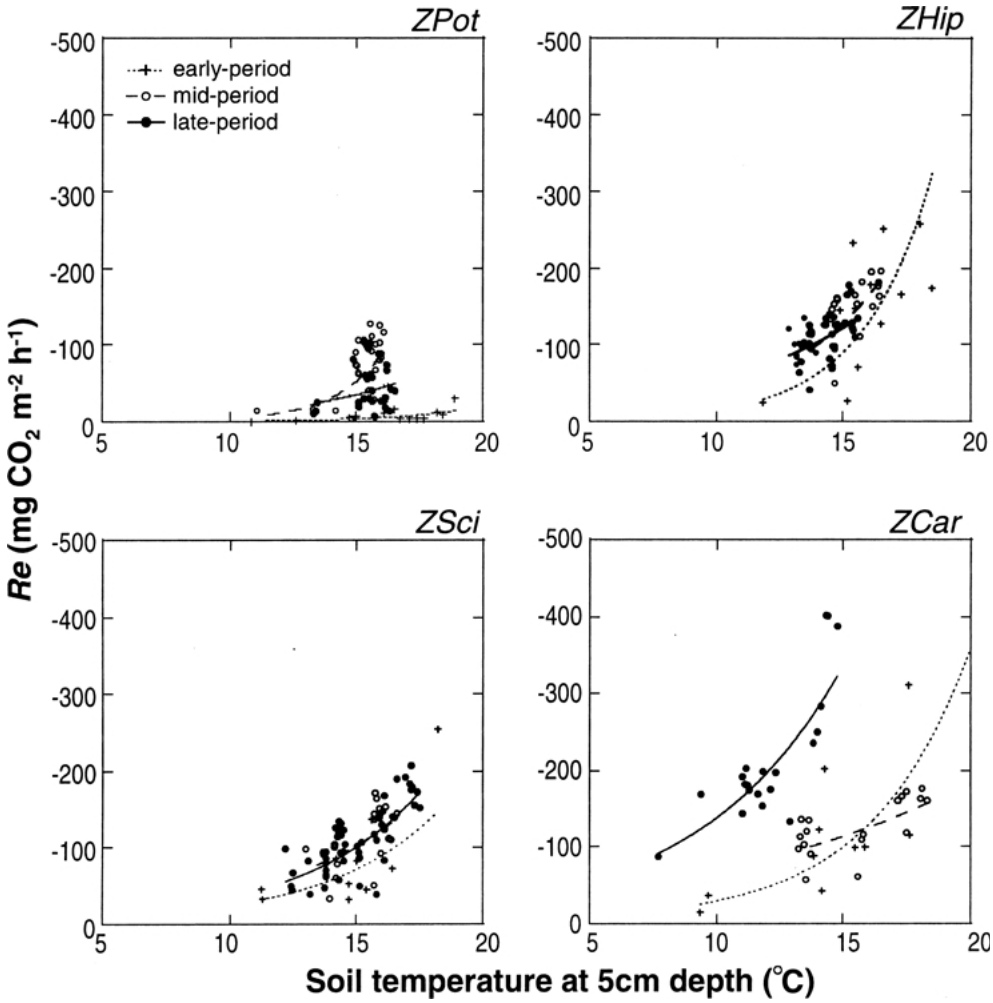

Figure 6. Relationship between soil temperature at a depth of 5 cm and ecosystem respiration (Re) in four vegetation zones. Early period: 4 to 26 July, mid-period: 27 July to 17 August, and late period: 17 August to 15 September. Curves were fitted using the exponential regression from Eq. (3). See Table 3 for a summary of parameter estimates.

Table 3. Ecosystem Respiration (Re) Parameters Fitted by an Exponential Curve

Period	Zone	Q_{10}	n	R^2
Early period	*ZPot*	8.1	13	0.73
	ZHip	8.9	12	0.70
	ZSci	6.0	13	0.83
	ZCar	7.6	15	0.88
Mid-period	*ZPot*	7.5	19	0.60
	ZHip	6.1	23	0.61
	ZSci	4.0	23	0.62
	ZCar	4.2	25	0.82
Late period	*ZPot*	2.0	29	0.48
	ZHip	3.3	29	0.66
	ZSci	5.1	30	0.73
	ZCar	2.8	34	0.67
Entire period	*ZPot*	5.1	61	0.52
	ZHip	2.7	64	0.44
	ZSci	3.2	66	0.51
	ZCar	2.8	74	0.55

Ranges of r^2 at $P < 0.005$ applicable for all parameters. Q_{10} represents change in Re rate over a 10°C range in soil temperature at 5 cm depth.

mated total Re was 36.8 g C m^{-2}, which yielded an estimated total NEP of 24.1 g C m^{-2}.

Discussion

Water Depth Plays a Key role in Wetland Carbon Dynamics

Small lakes and ponds are widely distributed on the Qinghai-Tibetan Plateau (Zhao 1999) and are often surrounded by highly developed deep-water wetlands. These wetlands are considered to play a critical role in the regional carbon dynamics of the world's highest plateau because of their high capacity for carbon storage. The Luanhaizi wetland was constantly submerged during the growing season, but exhibited marked spatial and temporal variation in water depth (Figure 2). Spatial variation in water depth is the major environmental factor causing vegetation zonation in this deep-water wetland, whereas seasonal variation in water depth affects the growth of vegetation. We there-

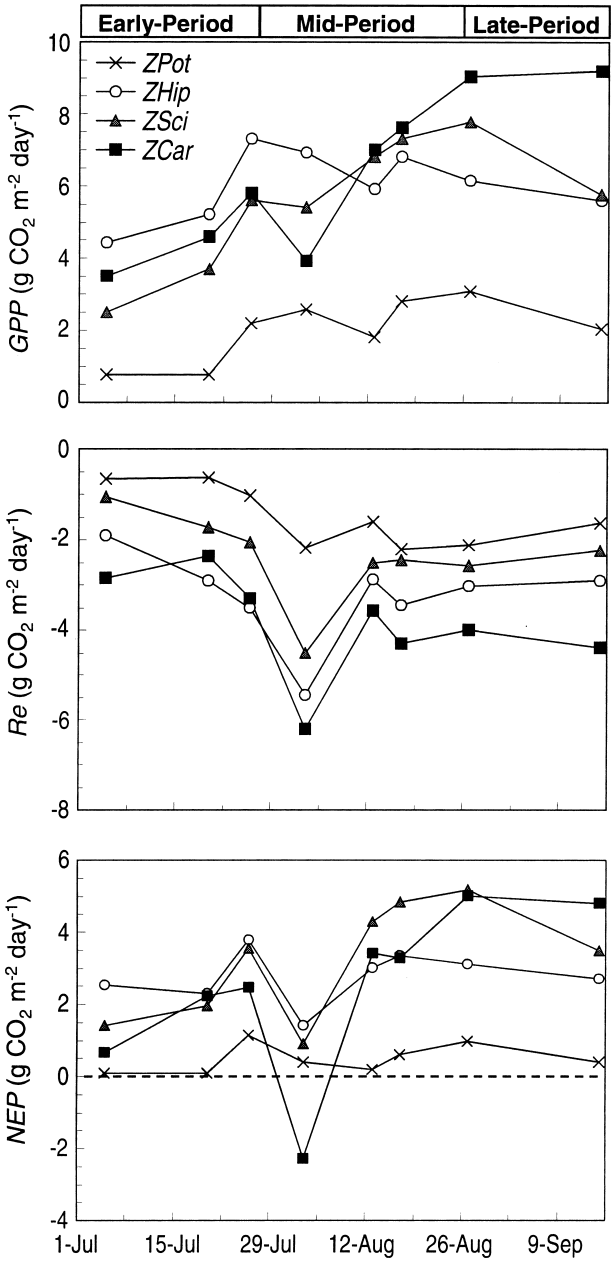

Figure 7. Seasonal variation in daily summed CO_2 fluxes, gross primary production GPP, Re, and NEP from 4 July to 15 September 2002. Positive values of NEP indicate CO_2 uptake and negative values indicate CO_2 emission.

fore hypothesized that water depth was one of the most critical environmental controls of carbon dynamics in this wetland. Stepwise regression confirmed that water depth was most strongly correlated with seasonal variation in CO_2 flux (Table 4). This was also supported by the observation of considerable variation in CO_2 flux caused by a short-term decrease in water depth (Figures 7 and 8).

Water depth may both directly and indirectly affect CO_2 dynamics in a wetland. Water depth directly alters the amount of aerial biomass, which is especially important under flooded conditions. The aerial tissue functions both as a gas conduit between the atmosphere and wetland soils via the plant roots, and in photosynthesis (for example, Cronk and Fennessy 2001). Hence, changes in aerial biomass will induce alterations in CO_2 uptake and emission by the emergent plants. A temporal increase in water depth would decrease ecosystem CO_2 uptake (GPP) and CO_2 emission (Re) mainly because of a decrease in the aerial, photosynthetic portion of the plants. We found that both Re and GPP decreased almost linearly with increasing water depth (Figure 8).

The indirect effect of water depth on carbon dynamics is more complicated. In the Luanhaizi wetland, vegetation dominated by *C. allivescers* V. Krez. occupied the shallowest zone, whereas the communities dominated by *S. distigmaticus* L, *H. vulgaris* L., and *P. pectinatus* L. occupied successively deeper zones (Figure 1, Table 1). Spatial variation in water depth strongly controlled vegetation zonation, and each zone consisted of different species of aquatic plants with specific structures and functions. Similar patterns of zonation along water depth gradients are reported for other wetlands and for littoral zones of lakes and seashores (Mitsch and Gosselink 2000). We found that CO_2 flux varied markedly among the vegetation zones, which are in turn affected by water depth. GPP, Re, and NEP also strongly depended on temporal variation in aboveground biomass of each vegetation zone (Figure 8), which is consistent with previous findings (Bubier and others 1998; Schreader and others 1998; Heikkinen and others 2002). Finally, water depth affects other environmental conditions, such as soil temperature, which decreased gradually from shallow to deep water (Figure 2). Because soil temperature affects Re (Figure 6), water depth may indirectly affect CO_2 flux by regulating soil temperatures.

A wetland ecosystem can be either a net CO_2 source or a net CO_2 sink depending on the water depth. Lakes with deep water have been reported as net CO_2 sources with CO_2 emission ranging from 1 to 169 g C m^{-2} over the ice-free season (Cole and Caraco 1998; Riera and others 1999; Casper and others 2000). Larmola and others (2003) demonstrated that the littoral zones of a boreal lake with a depth of up to 100 cm varied from a net CO_2 source (32 g C m^{-2} to a net CO_2 sink (101 g C m^{-2}) according to water depth. However, many high-latitude wetlands with low

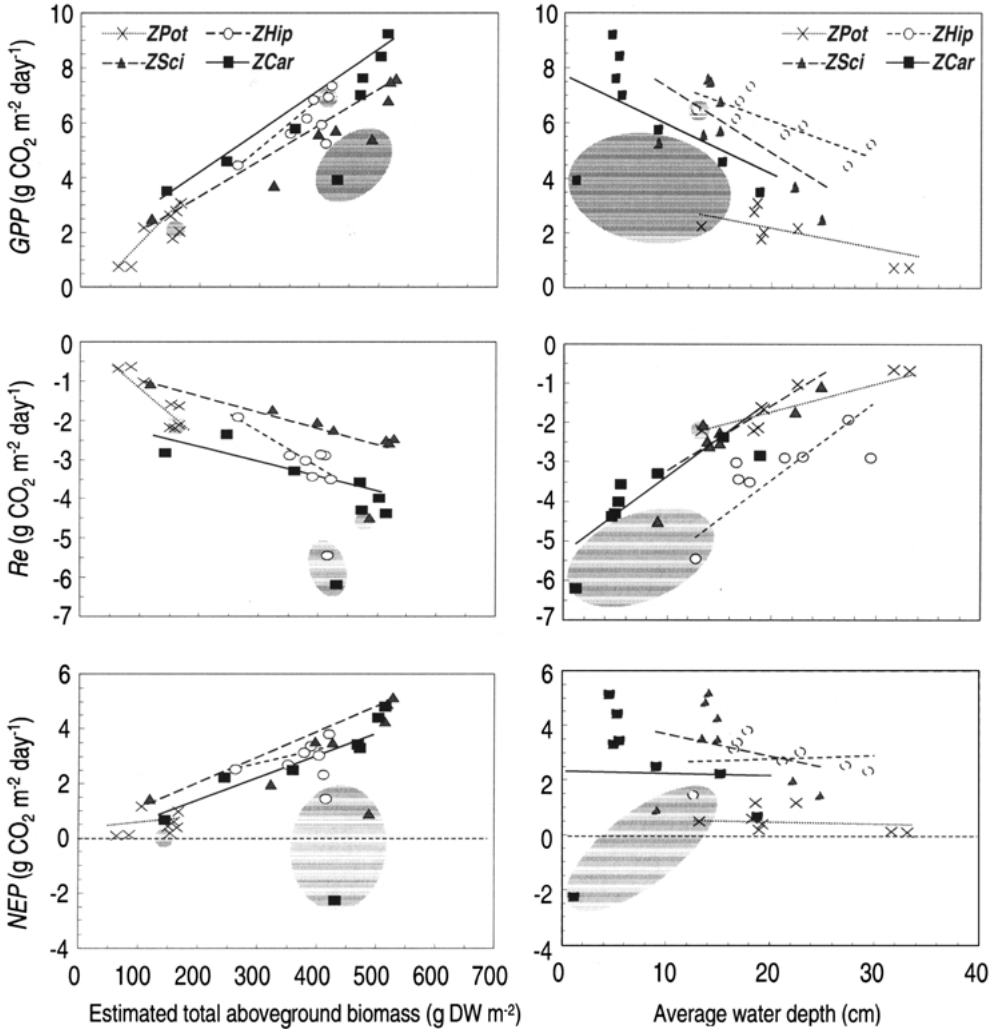

Figure 8. Relationships between CO_2 fluxes (GPP, Re, and NEP) and estimated total aboveground biomass (*left*) and relationships between CO_2 fluxes and water depth (*right*) for each vegetation zone. Data points within the *gray circle* were measured during the period of low water, 2, 3 August. Regression lines are linear fits with circled data excluded ($P < 0.01$). The regression equations are as follows. *Upper left*: $y = 0.0084x - 033$ ($R^2 = 0.85$) for *ZCar*, $y = 0.0091x - 0.078$ ($R^2 = 0.75$) for *ZSci*, $y = 0.0065x + 0.60$ ($R^2 = 0.78$) for *ZHip*, and $y = 0.0046x - 0.053$ ($R^2 = 0.37$) for *Zpot*; *middle left*: $y = -0.0043x - 1.8$ ($R^2 = 0.90$) for *ZCar*, $y = -0.0036x - 0.61$ ($R^2 = 0.98$) for *ZSci*, $y = 0.0094x + 0.53$ ($R^2 = 0.84$) for *ZHip*, and $y = -0.014x + 0.37$ ($R^2 = 0.91$) for *ZPot*; *lower left*: $y = 0.013x + 1.5$ ($R^2 = 0.96$) for *ZCar*, $y = 0.013x + 0.53$ ($R^2 = 0.93$) for *ZSci*, $y = 0.016x + 0.068$ ($R^2 = 0.73$) for *ZHip*, and $y = 0.019x - 0.43$ ($R^2 = 0.79$) for *ZPot*; *upper right*: $y = -0.17 + 4.3$ ($R^2 = 0.77$) for *ZCar*, $y = -0.22x + 7.1$ ($R^2 = 0.69$) for *ZSci*, $y = -0.054x + 4.2$ ($R^2 = 0.48$) for *ZHip*, and $y = -0.025x + 1.1$ ($R^2 = 0.26$) for *ZPot*; *middle right*: $y = 0.084x - 4.2$ ($R^2 = 0.60$) for *ZCar*, $y = 0.087x - 3.5$ ($R^2 = 0.78$) for *ZSci*, $y = 0.034x - 3.7$ ($R^2 = 0.24$) for *ZHip*, and $y = 0.072x - 3.0$ ($R^2 = 0.65$) for *ZPot*; *lower right*: $y = -0.25x + 8.4$ ($R^2 = 0.81$) for *ZCar*, $y = -0.30x + 11$ ($R^2 = 0.75$) for *ZSci*, $y = -0.088x + 7.8$ ($R^2 = 0.37$) for *ZHip*, and $y = -0.096x + 4.1$ ($R^2 = 0.59$) for *ZPot*.

water levels are reported as net CO_2 sinks over the growing season (Table 5). Our study suggests that the carbon budget of Luanhaizi wetland is somewhere between that of lakes and of high-latitude wetlands with shallow water (Table 1, Figure 9). If we assume that 5% of the Qinghai-Tibetan Plateau (Zhao 1999) is wetland with a NEP similar to that obtained in this study, a rough estimate of the net carbon sink would be 37.5 tons C (3.75×10^4 kg C) for the plateau wetland during the growing season only. However, a reliable estimate is difficult due to a lack of detailed information on the area, vegetation and growing seasonally for various wetlands on

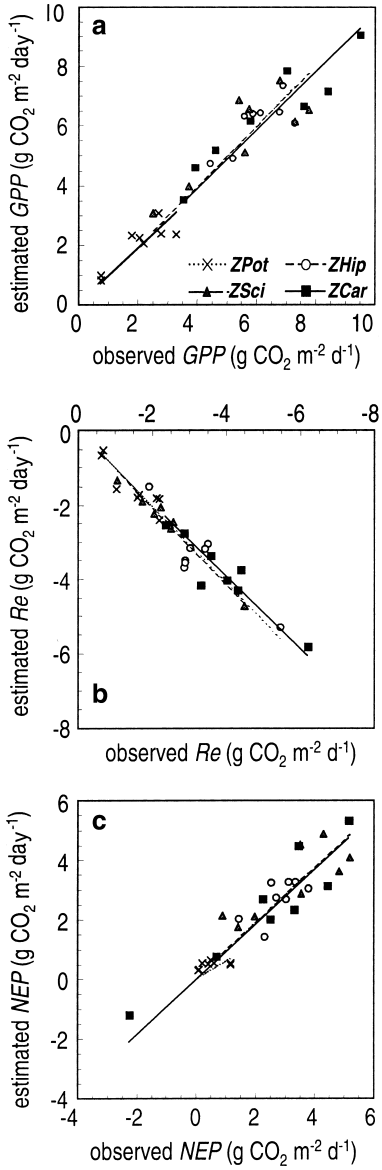

Figure 9. Comparison of daily summed values of (**a**) GPP, (**b**) Re, and (**c**) NEP predicted using stepwise regression (Table 4) with observed values from four vegetation zones.

the plateau. Moreover, long-term observation on wetland carbon dynamics is necessary for the extensive plateau.

Temperature Sensitivity of Ecosystem Respiration

In addition to water depth, temperature was another factor controlling CO_2 fluxes in the wetland (Table 2). Re was limited by soil temperature at a depth of 5 cm in all vegetation zones in the deep-water wetland (Figure 6). The strong temperature dependence of Re indicates that (1) soil temperature was the key factor for ecosystem respiration and (2) soil respiration may contribute noticeably to total ecosystem respiration.

Q_{10} is considered one of the most important parameters used to assess the temperature sensitivity of both soil and ecosystem respiration (Raich and Schlesinger 1992; Boone and others 1998). The global median of annual Q_{10} for soil respiration is reported as 2.4 (Raich and Schlesinger 1992). Q_{10} values for ecosystem respiration have been reported as between 3.0 and 4.1 in a boreal peatland and 1.6 and 2.2 in a northern peatland (Bubier and others 1998, 2003). Alpine and temperate wetlands had an estimated annual Q_{10} of 3.5 for ecosystem respiration (Wickland and others 2001; Carroll and Grill 1997). For the Luanhaizi wetland, we found a comparatively high Q_{10}, ranging from 2.0 to 8.9, and Q_{10} was much higher at the beginning of the growing season.

A high Q_{10} value measured in the field may reflect the influence of roots in controlling CO_2 emission. The Q_{10} of roots reaches 4.6 in forest soils, compared to 2.5 in root-free soil (Boone and others 1998). The dense root system and aboveground biomass in the wetland may contribute to the high Q_{10} we observed. Moreover, low temperature environments could also result in a high Q_{10}. The Q_{10} value is highest under low temperatures or in winter (Janssens and Pilegaard 2003). Hence, a high Q_{10} can be attributed to high plant root respiration and/or low soil respiration under low temperatures (Lloyd and Taylor 1994; Kirschbaun 1995). To elucidate the specific cause, further experimentation is needed.

PPFD Controls the Diurnal Pattern of CO_2 Flux

Daily variation in PPFD strongly affected the diurnal course of GPP and NEP. Parameters estimated from the non-linear rectangular regression between NEP and PPFD showed marked differences among vegetation zones, as well as among growth periods (Figure 5, Table 2). Variation of parameters among growth periods could be caused by changes in plant growth, water depth, and temperatures. Rapid changes over the growing season are a characteristic of CO_2 dynamics in high-altitude ecosystems, because environmental conditions and plant growth often vary dramatically during short growth periods (Körner 2003). In addition, NEP also showed large diurnal changes, with 100-fold changes NEP occurring within approximately 1 h in the early morning and late afternoon (Figure 4).

Table 4. Stepwise Multiple Regression for Daily Summed Re and GPP

Zone	Constant	*X*1	*X*2	*X*3	*X*4	r^2
Re = constant + X1 (PPFDave) + X2 (ATave) + X3 (STave) + X4(WD)						
ZPot	−3.482	–	–	–	0.089	0.80
ZHip	−6.44	0.015	–	−0.223	0.180	0.96
ZSci	−5.197	0.006	−0.138	–	0.182	0.92
ZCar	−0.258	–	–	−0.368	0.159	0.82
GPP = constant + X1 (PPFDave) + X2(ATave) + X3 (STave) + X4 (WD)						
ZPot	4.347	–	–	–	−0.106	0.58
ZHip	8.884	–	–	–	−0.143	0.51
ZSci	20.872	–	–	−0.715	−0.296	0.76
ZCar	13.037	–	−0.547	–	−0.177	0.75

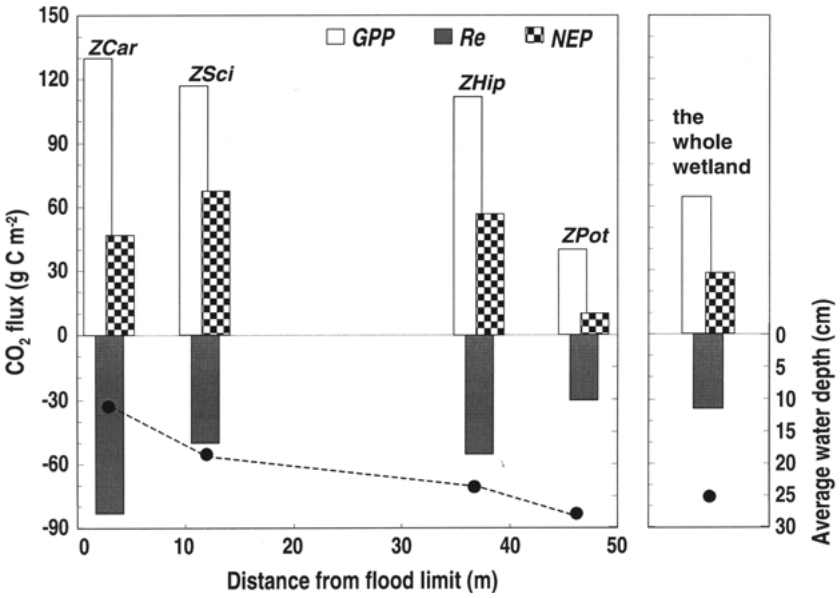

Figure 10. Summary of the seasonal CO_2 dynamics of each vegetation zone and of the entire wetland during the growing season of 2002 at an average water depth. CO_2 dynamics of the entire wetland were calculated using data on CO_2 dynamics and the occupied area of individual vegetation zones.

These changes in NEP could be attributed to rapid changes in PPFD.

ACKNOWLEDGEMENTS

This work was part of a joint research project by the National Institute for Environmental Studies, Japan, and the Northwest Plateau Institute of Biology, Chinese Academy of Sciences, and was supported by Asahi Breweries Scientific Foundation and a grant from the Knowledge Innovation Program of the Chinese Academy of Sciences (KZCX1-SW-01).

REFERENCES

Alm J, Talanov A, Saarnio S, Silvola J, Ikkonen E, Aaltonen H, Nykanen H, Martikainen PJ. 1997. Reconstruction of the carbon balance for microsites in a boreal oligotrophic pine fen, Finland. Oecologia 110:423–31.

Alm J, Schulman L, Walden J, Nykanen H, Martikainen PJ, Silvola J. 1999. Carbon balance of a boreal bog during a year with an exceptionally dry summer. Ecology 80:161–74.

Boone RD, Van Slycken J, Steven D. 1998. Roots exert a strong influence on the temperature sensitivity of soil respiration. Nature 396:570–72.

Bubier JL, Crill PM, Moore TR, Savage K, Varner RK. 1998. Seasonal patterns and controls on net ecosystem CO_2 exchange in a boreal peatland complex. Global Biogeochem Cycles 12:703–14.

Bubier JL, Frolking S, Crill PM, Linder E. 1999. Net ecosystem productivity and its uncertainty in a diverse boreal peatland. J Geophys Res Atmospheres 104:27683–92.

Bubier JL, Bhatia G, Moore TR, Roulet NT, Lafleur PM. 2003. Spatial and temporal variability in growing-season net ecosystem carbon dioxide exchange at a large peatland in Ontario, Canada. Ecosystems 6:353–67.

Table 5. Comparison of CO_2 Flux in Various Wetland Ecosystems during the Growing Season

Site Alpine wetland ecosystems	MAT (°C)	MAP (mm y^{-1})	MWD (cm)	Seasonal CO_2 flux (g C m^{-2}) GPP	Re	NEP	Hourly NEP (mg C $m^{-2}h^{-1}$)	AGB (g DW m^{-2})	Study period	References
Alpine wetland in Qinghai-Tibetan Plateau (N37/ E101, a.s.l. 3250m)	−2	500							Jul 1–Sep 15, 2002	This study
ZPot			27	40	−30	10	6	173		
ZHip			24	112	−55	57	37	415		
ZSci			19	118	−51	67	37	525		
ZCar			12	130	-83	47	28	515		
Whole the Lunanhaizi wetland				61	−37	24	13	263		
Alpine wetland at Rocky Mountain, USA (N40/W105, a.s.l 3200m)	0.5	120	3	280	−360	−80	–	218	1996–1998 (annual mean)	Wickland and others 2001
Boreal and arctic wetland ecosystems										
Zackenberg, Greenland (N74/W21, a.s.l. ND)	−9.2	223							Jul–Sep, 1997	Christensen and others 2000
Cassiope heath			–	–	–	–	6	267		
Hummock fen			−11	–	–	–	52	203		
Grassland			−4	–	–	–	55	207		
Hollow			−7	–	–	–	13	268		
Safix arctica			1	–	–	–	42	88		
European tundra, Russia (N67/E63, a.s.l. ND)	−6.0	548							Jul–Sep, 1999	Heikkinen and others 2002
Wet flask			>0	68	−37	25	44	–		
Intermidiate flarks			−5∼0	131	−77	49	75	–		
Wet lawn			−10∼−5	176	−126	45	76	–		
Intermidiate Lawns			−10∼−20	164	−129	34	64	–		
Boreal peatland in a northen Sweden (N63/E20, a.s.l. 35m)	2.3	590								Waddington and Roulet 2000
Intermidiate lawn			−3	117	−110	16	–	–	Jun–Sep, l992	
Intermidiate ridge			−30	210	−191	19	–	–		
Intermidiate lawn			−0	220	−202	18	–	–	Jun–Sep, 1993	
Intermidiate ridge			−22	302	-278	24	–	–		
Lek Vorkuta catchment, Eastern Russia (N67/E63, a.s.l. ND)	−5.9	548							Jun–Sep, 2001	Heikkinen and others 2004
Sphagnum dominated peat Ombrotrophic bog			−4	204	−232	−28	−6	420		

Site Alpine wetland ecosystems	MAT (°C)	MAP (mm y^{-1})	MWD (cm)	Seasonal CO_2 flux (g C m^{-2}) GPP	Re	NEP	Hourly NEP (mg C $m^{-2}h^{-1}$)	AGB (g DW m^{-2})	Study period	References
Intermediate flarks			−4	217	−93	129	84	520		
Hummocks			< −20	194	−317	−123	−32	550		
Lake and pond margins			10	325	−325	0	60	240		
Mirabel peatland, Quebec, Canada (N45/W73, a.s.l. ND)	6.1	940	−29	254	129	125	–	–	Apr–Nov, 1997	Roehm and Roulet 2003
Salmisuo fen, Finland (N67/E30, a.s.l. ND)	1.9	648							May–Sep, 1993	Alm and others 1997
Flask			−2	225	−110	135	–	–		
Eriophorum lawn			−5	300	−140	160	–	–		
Carex lawn			−3	317	−164	153	–	–		
Hummock			−23	314	−206	108	–	–		
Whole mire				302	−149	153	–	–		
Ahvensalo bog, Finland (N62/E30, a.s.l. ND)	2.0	ND							May–Sep, 1994	Alm and others 1999
Hollow			−5	188	−198	−10	–	–		
Sphragnum ang Lawn			−7	235	−194	41	–	–		
Sphragnum fuscum Lawn			−15	209	−255	−46	–	–		
Hummock			<−25	171	−288	−117	–	–		
Whole mire				205	−255	−50	–	–		
Littoral zone of boreal eutrophic lake Finland (N63/E27, a.s.l. ND)	ND	ND							Mid-Mid–Oct 1998 (wetter year)	Larmola and others 2003
Flooded meadow			10	641	−672	−32	–	84		
Marsh			27	314	−264	22	–	77		
Phragmites stand			77	49	−51	−2.5	–	31		
Nupher stand			100	–	–	−5	–	10		
Flooded meadow			−29	856	−821	35	–	300	Mid-May–Oct, 1999 (dner year)	
Marsh			−12	504	−403	101	–	180		
Phragmites stand			38	69	−64	5	–	14		
Nupher stand			61	–	–	34	–	26		

Bubier JL, Crill P, Mosedale A, Frolking S, Linder E. 2003b. Peatland responses to varying interannual moisture conditions as measured by automatic CO_2 chambers. Global Biogeochemical Cycles 17:1066, doi: 10.1029/2002GB001946.

Carroll P, Crill P. 1997. Carbon balance of a temperate poor fen. Global Biogeochem Cycles 11:349–56.

Casper P, Maberly SC, Hall GH, Finlay BJ. 2000. Fluxes of methane and carbon dioxide from a small productive lake to the atmosphere. Biogeochemistry 49:1–19.

Christensen TR, Friborg T, Sommerkorn M, Kaplan J, Illeris L, Soegaard H, Nordstroem C, Jonasson S. 2000. Trace gas exchange in a high-arctic valley 1. Variations in CO_2 and CH_4 flux between tundra vegetation types. Global Biogeochem Cycles 14:701–13.

Cole JJ, Caraco NF, Kling GW, Kratz TK. 1994. Carbon dioxide supersaturation in the surface waters of lakes. Science 265:1568–70.

Cole JJ, Caraco NF. 1998. Atmospheric exchange of carbon dioxide in a low-wind oligotrophic lake measured by addition of SF6. Limnol Oceanogr 43:647–56.

Cowardin LM, Carter V, Golet FC, LaRoe ET. 1979. Classification of wetlands and deepwater habitats of the United States. FWS/OBS-79-31. United States Department of the Interior Fish and Wildlife Service, Washington (DC): 103 p.

Cronk JK, Fennessy MS. 2001. Adaptations to growth conditions in wetland. Wetland plants: biology and ecology. Boca Raton (FL): Lewis Publishers. p 87–110.

Gorham E. 1991. Northern peatlands – role in the carbon-cycle and probable responses to climatic warming. Ecol Appl 1:182–95.

Heikkinen JEP, Elsakov V, Martikainen PJ. 2002. Carbon dioxide and methane dynamics and annual carbon balance in tundra wetland in NE Europe, Russia. Global Biogeochem Cycles 16:1115, doi: 10.1029/2002GB001930.

Heikkinen JEP, Virtanen T, Huttunen JT, Elsakov V, Martikainen PJ. 2004. Carbon balance in East European tundra. Global Biogeochemical Cycles 18, GB1023, doi: 10.1029/2003GB002054.

Hirota M, Tang YH, Hu QW, Hirata S, Kato T, Mo WH, Cao GM, Mariko S. 2004. Methane emissions from different vegetation zones in a Qinghai-Tibetan Plateau wetland. Soil Biol Biochem 36:737–48.

IPCC. 2001. Climate Change 2001. Third Assessment Report of the IPCC. Cambridge: Cambridge University Press, p 183–237.

Janssens IA, Pilegaard K. 2003. Large seasonal changes in Q_{10} of soil respiration in a beech forest. Global Change Biol 9:911–88.

Joiner DW, Lafleur PM, McCaughey JH, Bartlett PA. 1999. Interannual variability in carbon dioxide exchanges at a boreal wetland in the BOREAS northern study area. Journal of Geophysical Research-Atmospheres 104:27663–72.

Kirschbaum MUF. 1995. The temperature dependence of soil organic matter decomposition, and the effect of global warming on soil organic C storage. Soil Biol Biochem 36:753–760.

Körner C. 2003. Alpine Plant Life, Functional Plant Ecology of High Mountain Ecosystems. Second Edition. Springer: New York.

Larmola T, Alm J, Juutinen S, Saarnio S, Martikainen PJ, Silvola J. 2003. Floods can cause large interannual differences in littoral net ecosystem productivity. Limnology and Oceanography 49:1896–1906.

Lloyd J, Taylor JA. 1994. On the temperature dependence of soil respiration. Funct Ecol 8:315–323.

Mitsch WJ, Gosselink JG. 2000. Wetlands. Third edition. John Wiley and Sons: New York.

Moore TR, Dalva M. 1993. The influence of temperature and water-table position on carbon dioxide and methane emissions from laboratory columns of peatland soils. J Soil Sci 44:651–64.

Oechel WC, Hastings SJ, Vourlitis G, Jenkins M, Riechers G, Grulke N. 1993. Recent change of arctic tundra ecosystems from a net carbon dioxide sink to a source. Nature 361:520–23.

Raich JW, Schlesinger WH. 1992. The global carbon dioxide flux in soil respiration and its relationship to vegetation and climate. Tellus 44B:81–90.

Riera JL, Schindler JE, Kratz TK. 1999. Seasonal dynamics of carbon dioxide and methane in two clear-water lakes and two bog lakes in northern Wisconsin, USA. Can J Fish Aquat Sci 56:265–74.

Roehm CL, Roulet NT. 2003, Seasonal contribution of CO2 fluxes in the annual C budget of a northern bog. Global Biogeochem Cycles 17: GB1029, doi: 10.1029/2002GB001889.

Schreader CP, Rouse WR, Griffis TJ, Boudreau LD, Blanken PD. 1998. Carbon dioxide fluxes in a northern fen during a hot, dry summer. Global Biogeochem Cycles 12:729–40.

Silvola J, Alm J, Ahlholm U, Nykanen H, Martikainen PJ. 1996. CO_2 fluxes from peat in boreal mires under varying temperature and moisture conditions. J Ecol 84:219–28.

Thornley MN, Johnson IR. 1990. Plant and crop modeling; a mathematical approach to plant and crop physiology. Oxford: Clarendon.

Trumbore SE, Bubier JL, Harden JW, Crill PM. 1999. Carbon cycling in boreal wetlands: a comparison of three approaches. J Geophys Res Atmos 104:27673–82.

Turunen J, Tomppo E, Tolonen K, Reinikainen A. 2002. Estimating carbon accumulation rates of undrained mires in Finland – application to boreal and subarctic regions. Holocene 12:69–80.

Vollenweider RA. 1968. The scientific basis of lake and stream eutrophication with particular reference to phosphorus and nitrogen as eutrophication factors. Technical Report DAS/CSI/68,27, Paris: Organization of Economic Cooperation and Development.

Waddington JM, Roulet NT. 1996. Atmosphere-wetland carbon exchanges: scale dependency of CO_2 and CH_4 exchange on the developmental topography of a peatland. Global Biogeochem Cycles 10:233–45.

Waddington JM, Roulet NT. 2000. Carbon balance of a boreal patterned peatland. Glob Change Biol 6:87–97.

Wang G, Qian J, Cheng G, Lai Y. 2002. Soil organic carbon pool of grassland soils on the Qinghai-Tibetan Plateau and its global implication. Sci Total Environ 291:207–17.

Wickland KP, Striegl RG, Mast MA, Clow DW. 2001. Carbon gas exchange at a southern Rocky Mountain wetland, 1996–1998. Global Biogeochem Cycles 15:321–35.

Zhao K. 1999. Marshes and swamps of China; a compilation. Science Press of China. (In Chinese only).